JJMIE

Volume 13, Number 2, July. 2019
ISSN 1995-6665
Pages 69 - 74

Jordan Journal of Mechanical and Industrial Engineering

A New Analytical Approach for Crack Modeling in Spur Gears

Ehsan Rezaei, Mehrdad Poursina*, Mohsen Rezaei, Alireza Ariaei

Department of Mechanical Engineering, Faculty of Engineering, University of Isfahan, Isfahan, 81744-73441, Iran

Received 10 April. 2019

Abstract

Spur gear systems are widely used in power transmission systems in the industry. One of the common defects of the gears is tooth crack. Tooth crack increases the vibration and also generates noise. Previous studies have shown that tooth stiffness will decrease due to any crack and it is important to estimate the magnitude of reduction of tooth stiffness. This research suggests a new analytical approach for crack modeling and determining the reduction of time-varying gear mesh stiffness by Elastic Spring Method (ESM). Based on this approach, two or more cracks can be considered in one tooth. However, previous studies have primarily concentrated on one crack. In addition, it should be voted that each crack is replaced by one linear and one torsional spring in the present study. The results that were obtained from this method are validated through a comparison with Limit Line Method (LLM) and Finite Element Method (FEM).

Keywords: Spur Gear - Tooth Crack – Mesh Stiffness –Analytical Approach- Finite Element Method;

1. Introduction

Like other components in the industry, gears which are made of teeth are subject to certain damages. Tooth crack is an unwanted phenomenon, and can cause serious and costly damages. Time-varying mesh stiffness is the main reason of vibration in gears [1]. There exist some studies on assessing mesh stiffness. The FEM [2, 3] and Analytical Method (AM) have been and are being applied for computing mesh stiffness. Wang and Howard [4] applied FEM to compute the torsional stiffness of a spur gear pair. Weber [5] and Cornell [6] applied AM to calculate the gear mesh stiffness, while Kasuba and Evans [7] computed the same through a digitization approach. Yang and Lin [8] calculated the mesh stiffness of spur gears through the potential energy method by considering bending, axial compressive and Hertzian energy.

The existence of the cracks in the gear teeth is considered as stiffness reduction. The most common method applied in reducing modulus of elasticity at crack location [9]. The effect of the crack propagation size on the mesh stiffness is studied by Tian [10]. Wu et al. [11] assessed this effect on the dynamic response of a gearbox. Pandya and Parey [12, 13] assessed the effect of the crack path on mesh stiffness subject to different gear parameters, such as pressure angle, fillet radius, contact ratio, and backup ratio.

An analytical approach is presented by Chaari [14] to evaluate reduction in total gear mesh stiffness due to crack propagation, and a FEM model is used to verify the results obtained in an analytic manner. A modified mathematical model is proposed by Zhou [15] on crack growth in the tooth root. Two additional scenarios of (a constant crack depth with a varying crack length and a constant crack length with a varying crack depth) for cracks are presented by Chen & Shao [16]. An analytical approach to calculate the mesh stiffness and model the crack propagation with a non-uniform parabolic path depth is proposed by Mohammad [17].

Liming and Yimin [18] studied the effect of tooth root crack on the mesh stiffness and dynamic response of spur gear pair considering a half-sinusoidal function for crack propagation path based on the real crack profile. Zaigang et al. [19] assessed the effect of crack on the fillet-foundation stiffness of gear and by comparison with FEM result proved that the load carrying zone depends on the tooth root crack depth in calculating the fillet-foundation stiffness. Wu et al. [20] studied the effect of tooth root crack on the mesh stiffness and dynamic response of spur gear system by LLM and FEM and compared their results with the experimental signals.

In the most available studies, the LLM is applied to reduce tooth thickness and calculating the total mesh stiffness, where considering two or more cracks in one tooth is impossible. In the method presented here, by defining torsional and linear springs instead of the cracks, two or more cracks with constant or variable crack depths through the whole tooth width or any length at any location of the tooth can be modeled.

2. Mathematical Model

This section contains two subsections, the first is the mesh stiffness analytical calculation and the latter is a new approach for the crack modeling in the mesh stiffness.

* Corresponding author e-mail: poursina@eng.ui.ac.ir.

2.1. Analytical Calculation of Mesh stiffness

The mesh stiffness analytical calculation is the most known and repeatedly explained method, but it is necessary to mention it here before proposing the new crack modeling approach. Mesh stiffness is a parameter subject to gear parameters such as module, number of teeth, pressure angle, face width, hub bore radius and material properties. The stiffness of a pair of teeth (single mesh) is obtained by calculating bending (k_b), shear (k_s), axial (k_a), fillet-foundation stiffness (k_f) of each tooth and contact stiffness (k_h) of the teeth as Eqs. (1) to (5) [21]:

$$\frac{1}{K_h} = \frac{4(1-\nu^2)}{\pi E L} \tag{1}$$

$$\frac{1}{k_b} = \int_0^d \frac{((d-x)\cos(a_m) - h\sin(a_m))^2}{E\, I_x}\, dx \tag{2}$$

$$\frac{1}{k_s} = \int_0^d \frac{1.2\, cos^2(a_m)}{G\, A_x}\, dx \tag{3}$$

$$\frac{1}{k_a} = \int_0^d \frac{sin^2(a_m)}{E\, A_x}\, dx \tag{4}$$

$$\frac{1}{K_f} = \frac{cos^2(a_m)}{L.E}\left[L^*\left(\frac{u_f}{S_f}\right)^2 + M^*\left(\frac{u_f}{S_f}\right) + P^*\left(1 + Q^*\, tan^2(a_m)\right)\right] \tag{5}$$

where, h, α_m, x, dx and d are defined in Fig. 1; E, G, and υ are the Young's modulus, shear modulus and Poisson's ratio of gear material respectively. L is the gear face width; A_x is the tooth section area at point x measured from $A_x = (2h_x)L$; and I_x is the moment inertia of tooth section area at point x measured through $I_x = \frac{1}{12}(2h_x)^3 L = \frac{2}{3}{h_x}^3 L$; the definition of u_f and S_f , L^*,M^*, P^* and Q^* are presented in [22].

After calculating the stiffness for pinion and gear, total single stiffness (K_e) is calculated as Eq.(6) [21]:

$$K_e = \frac{1}{\frac{1}{K_{ap}} + \frac{1}{K_{bp}} + \frac{1}{K_{sp}} + \frac{1}{K_{fp}} + \frac{1}{K_h} + \frac{1}{K_{ag}} + \frac{1}{K_{bg}} + \frac{1}{K_{sg}} + \frac{1}{K_{fg}}} \tag{6}$$

where the first four terms relate to pinion and the last four terms related to gear.

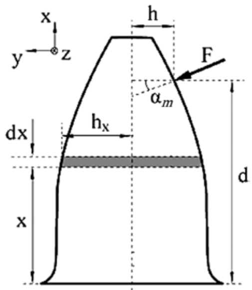

Figure 1. Tooth parameters

2.2. Analytical Crack Model

The issue of crack in the tooth root is the focus of many studies. The crack originates from freedom circle and extends to the center of the tooth on the root and then extends to other side of the tooth in a symmetric manner. In general, the types of cracks in the root are of two categories (Fig. 2):

1. Overall crack with constant depth
2. Non-overall crack with varying depth

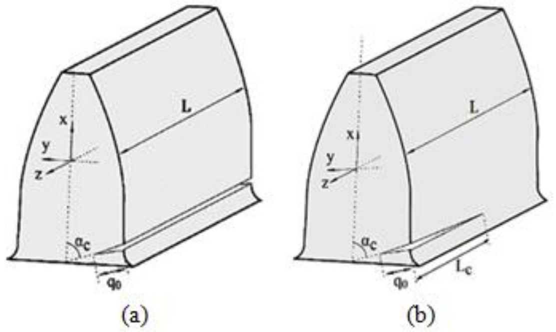

Figure 2. Cracked tooth (a) Overall crack with constant depth (b) Non-overall crack with varying depth

For modeling and calculating stiffness reduction of the cracked tooth, equivalent springs are applied. In this application the subject tooth is divided into two parts at the crack location, and the crack is replaced by linear and torsional springs, Fig. 3, subjected to a specified force and torque respectively. The stiffness of the springs are related to the depth of the crack and the thickness of the tooth in the crack region. In this model, the linear spring undergoes the shear force and torsional spring becomes subject to flexural torque. To assemble the linear and torsional springs, it is necessary to convert the angular deflection of the torsional spring to linear deflection by multiply it in the corresponding arm. After calculating the deflection due to rotation of torsional spring (δ_t) and the deflection of linear spring (δ_l) by Eqs. (7) and (8), their stiffness can be calculated as Eq. (9):

$$\delta_t = \frac{2\, h_c}{E\ A_c}\, q_t(\lambda)\, (F.u^2 \cos\alpha_m - F.h^2 \sin\alpha_m) \tag{7}$$

$$\delta_l = \frac{2\, F\, h_c}{E\, I_c}\, q_l(\lambda) \cos\alpha_m \tag{8}$$

$$k_t = \frac{F}{\delta_t}\,,\ \ k_l = \frac{F}{\delta_l} \tag{9}$$

where, h, u and F are defined in Fig. 3; k_l and k_t are the linear and torsional spring stiffness respectively, h_c is the width of the tooth; A_c and I_c are area and area moment of inertia in the crack section respectively.

$q_t(\lambda)$ and $q_l(\lambda)$ are the functions related to the crack depth ratio that for the tooth with a rectangular section are expressed by Eq.(10) and (11) [23]:

$$q_t(\lambda) = \left(\frac{\lambda}{1-\lambda}\right)^2 \left(0.99 - \lambda(1-\lambda)(1.3 - 1.2\lambda + 0.7\lambda^2)\right) \tag{10}$$

$$q_l(\lambda) = \left(\frac{\lambda}{1-\lambda}\right)^2 (5.93 - 19.69\,\lambda + 37.14\,\lambda^2 - 35.84\,\lambda^3 + 13.12\,\lambda^4) \tag{11}$$

where, λ is the crack depth ratio and calculated by Eq.(12):

$$\lambda = \frac{q_c \sin\alpha_c}{h_c} \tag{12}$$

After calculating k_l and k_t the total mesh stiffness is expressed by Eq(13):

$$K_e = \frac{1}{\frac{1}{K_{ap}} + \frac{1}{K_{bp}} + \frac{1}{K_{sp}} + \frac{1}{K_{fp}} + \frac{1}{K_h} + \frac{1}{K_{ag}} + \frac{1}{K_{bg}} + \frac{1}{K_{sg}} + \frac{1}{K_{fg}} + \frac{1}{K_{tp}} + \frac{1}{K_{lp}}} \quad (13)$$

where, k_{tp} and k_{lp} are the stiffness of the equivalent springs on the pinion.

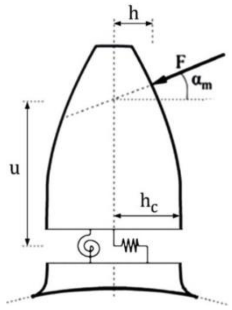

Figure 3. Cracked tooth model with torsional and linear spring

2.2.1. Tooth with two cracks

A tooth with two cracks is modeled in Fig. 4 where the mentioned springs are applied. The first crack is in tooth root, and the other is in pitch circle. At pitch location, when load position is below the crack location, no stiffness reduction takes place, while, when load position is above the crack location, the tooth is divided into three slices and the same calculation for stiffness reduction is made. After calculating K_t and K_l for the first and second cracks using Eqs. (14) and (15), the total mesh stiffness is calculated through Eq. (16):

$$\frac{1}{K_t} = \frac{1}{K_{t1}} + \frac{1}{K_{t2}} \quad (14)$$

$$\frac{1}{K_l} = \frac{1}{K_{l1}} + \frac{1}{K_{l2}} \quad (15)$$

$$K_{e1} = \frac{1}{\frac{1}{K_{ap}} + \frac{1}{K_{bp}} + \frac{1}{K_{sp}} + \frac{1}{K_{fp}} + \frac{1}{K_h} + \frac{1}{K_{ag}} + \frac{1}{K_{bg}} + \frac{1}{K_{sg}} + \frac{1}{K_{fg}} + \frac{1}{K_{tp}} + \frac{1}{K_{lp}}} \quad (16)$$

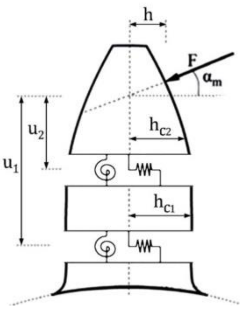

Figure 2. Modeling of the tooth with two cracks

2.2.2. Tooth with varying crack depths

A tooth with one crack that its depth ($q(z)$) follows a parabolic function along the tooth width shown in Fig. 5. When the crack length is less than the whole tooth width the following holds true (Eq.(17)) [21]:

$$\begin{cases} q(z) = q_0 \sqrt{\frac{w_c - z}{w_c}} & 0 < z < w_c \\ q(z) = 0 & z \geq w_c \end{cases} \quad (17)$$

where, w is the tooth width, w_c is the crack length, and q_0 is the maximum crack depth (Fig. 5). When the crack length extends through the tooth width the following holds true (Eq. (18)):

$$q(z) = \sqrt{\frac{q_0^2 - q_2^2}{L} z + q_2^2} \quad (18)$$

To obtain the stiffness reduction for tooth with varying crack depths, the tooth face is divided into many slices and the previous equation are applied to calculate the crack depth in each slice. Then, the equivalent springs are modeled in each slice and whole stiffness of springs in all slices is obtained by adding all of them.

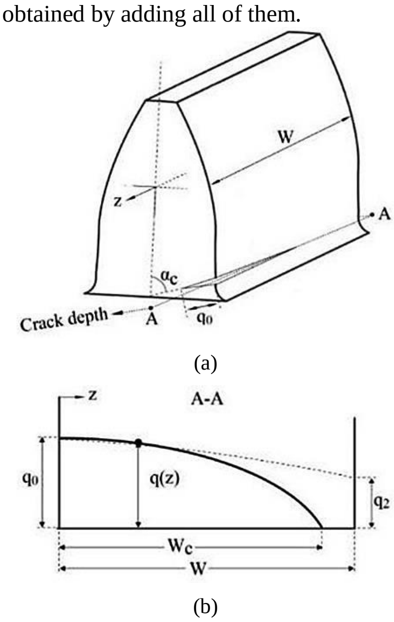

Figure 5. Modeling of gear tooth crack with non-uniform distribution. (a) Modeling of the cracked tooth, (b) crack depth distribution along the tooth width [21]

3. Result and discussion

To verify this proposed approach, a single stage gearbox is considered like that of [21]. The gear parameters are presented in Table 1, through which three examples are solved.

Table 1. Gear parameters [21]

Parameters	pinion	gear
Number of teeth	30	25
Module (mm)	2	2
Tooth width (mm)	20	20
Contact ratio	1.63	1.63
Pressure angle (deg.)	20	20
Young′s modulus (GPa)	200	200
Poisson′s ratio	0.3	0.3

The mesh stiffness results for different crack sizes that are mentioned in Table 2, drawn by Mohammed [21] are shown in Fig. 6-a, and the present results are shown in Fig. 6-b. It is obvious that the change patterns in both diagrams are similar and the values are the same approximately. The maximum difference is in 1.8 mm crack size with about 3 % difference.

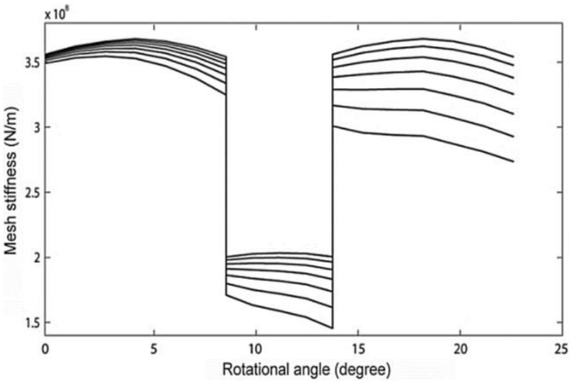

(a)

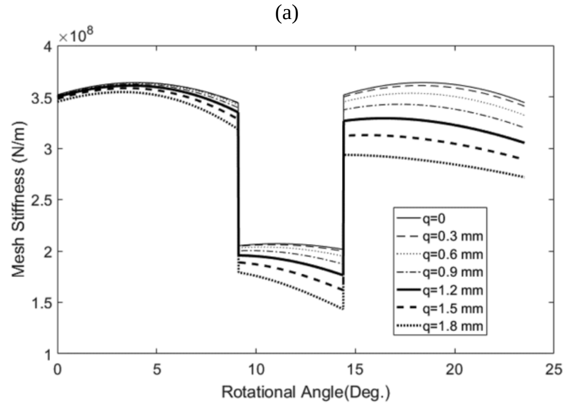

(b)

Figure 3. Time-varying gear-mesh stiffness for crack with constant depth (a) obtained by Mohammed [21] and (b) obtained in this study

Table 2. Data for crack with constant depth [21]

Case	$q_0\ (mm)$	CL %	
1	0	0	
2	0.3	8.06	
3	0.6	16.12	
4	0.9	24.19	$\alpha_c = 70^{\circ}$
5	1.2	32.25	
6	1.5	40.32	
7	1.8	48.38	

In the second example, the results of the crack with non-uniform depth are compared with the results of Mohammed [24]. The result presented in Fig. 7 indicates a good agreement and validates the approach developed in this study. Crack properties of the driven gear are tabulated in Table 3.

Table 3. Data for crack with non-uniform depth [24]

Case	$q_0\ (mm)$	$w_c\ (mm)$	$q_2\ (mm)$	
1	0	0	0	
2	0.2	5	0	
3	0.4	10	0	
4	0.6	15	0	
5	0.8	20	0	$\alpha_c = 70^{\circ}$
6	1.0	20	0.45	
7	1.2	20	0.7	
8	1.4	20	0.925	
9	1.6	20	1.14	

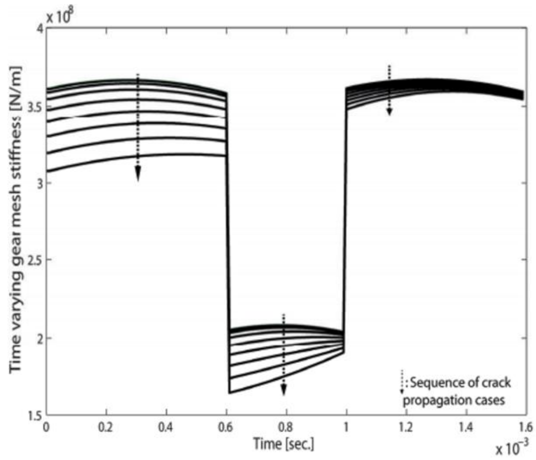

(a)

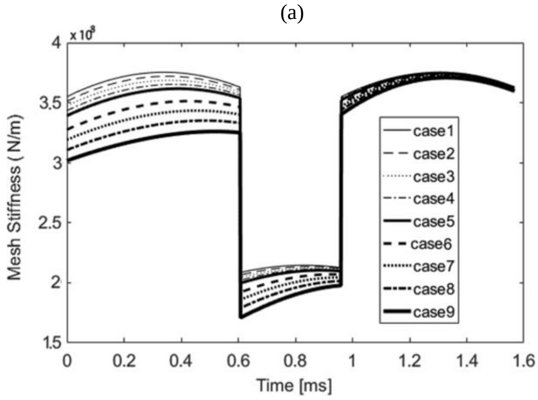

(b)

Figure 7. Time-varying mesh stiffness for non-uniform depth cracks (a) LLM used by Mohammed [24] and (b) ESM

In the third example, a tooth with two cracks as shown in Fig. 4 is of concern. The first crack is at tooth root and the second is at the pitch circle. Crack properties are tabulated in Table 4. The limit line method is unable to model two cracks in one tooth. So, the result of the proposed method is compared with the FEM. This example is modeled and simulated in Abaqus software by dynamic implicit solution method in plain stress condition and the cracks are modeled by the contour integral method. The element shapes and the meshing method that is used in the gears whole body is mesh quad free, except the cracks tip regions in the pinion tooth that mesh quad-dominated sweep is used. The numbers of elements in pinion and gear are 3211 and 5974 respectively. The element type was standard - Linear and contact defined as surface to surface with frictionless tangential behavior. The stress contour of modeled gears with only one tooth in contact is shown in Fig.8.

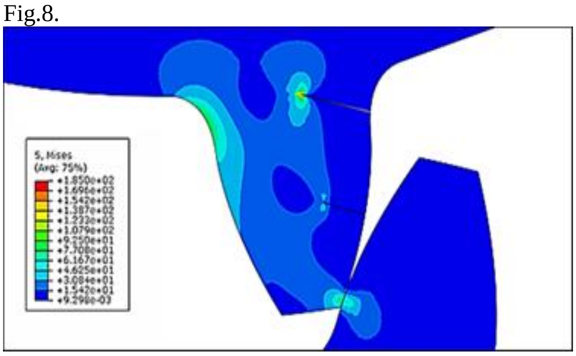

Figure 8. FEM Model

When the contact point is below the second crack zone, no reduction takes place. When the crack length in tooth root increases, the influence of the second crack will be decreased, a careful observation of Fig. 9 will prove this claim.

Table 4. data for two cracks

Case	Root Crack $q_1\ (mm)$	Pitch Crack $q_2\ (mm)$	
1	0	0	$\alpha_c = 70^{\circ}$
2	0	1	
3	1.8	0	
4	1.8	1	

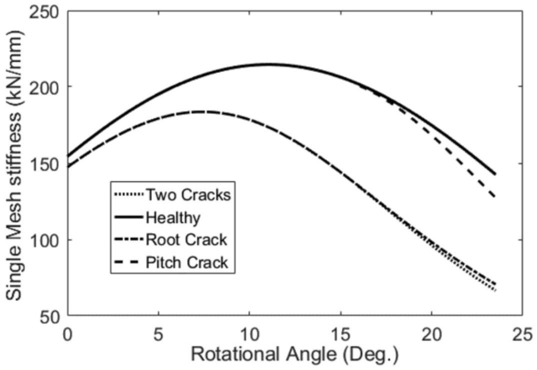

(a)

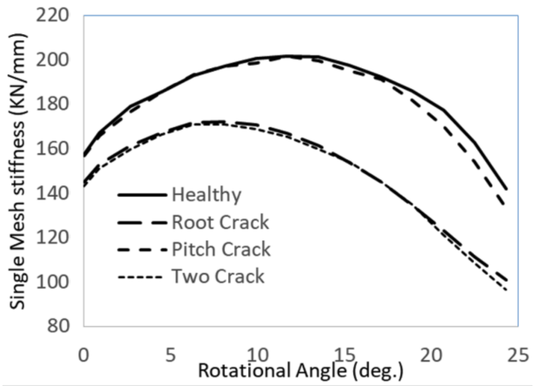

(b)

Figure 9. Single mesh stiffness for a tooth with two cracks (a) AM result (b) FEM result

4. Conclusions

The results of this investigation show that the modeling two cracks in one tooth are obtainable by this newly proposed approach (ESM). In contrast, it was impossible according to previous studies. When the cracked tooth is in mesh, the influence of the crack decreases the gear mesh stiffness. Furthermore, the effect of a tooth crack on its stiffness is modeled by adding torsional and linear springs at the crack location. The recent approach results of single mesh stiffness in the case of two cracks in one tooth at the root and the pitch circles are compared with the FEM and showed the good agreement.The evidence from this study suggests that the obtained time-varying gear mesh stiffness can be applied in checking the dynamic behavior of the gear in the presence of the crack.

References

[1] Lin, Jian, and Robert G. Parker. "Mesh stiffness variation instabilities in two-stage gear systems." Journal of vibration and acoustics 124, no. 1 (2002): 68-76.

[2] Sirichai, Seney. "Torsional properties of spur gears in mesh using nonlinear finite element analysis." PhD diss., Curtin University, 1999.

[3] Pimsarn, Monsak, and Kazem Kazerounian. "Efficient evaluation of spur gear tooth mesh load using pseudo-interference stiffness estimation method." Mechanism and machine theory 37, no. 8 (2002): 769-786.

[4] Wang, Jiande, and Ian Howard. "The torsional stiffness of involute spur gears." Proceedings of the Institution of Mechanical Engineers, Part C: Journal of Mechanical Engineering Science 218, no. 1 (2004): 131-142.

[5] Cornell, R. W. "Compliance and stress sensitivity of spur gear teeth." Journal of Mechanical Design 103, no. 2 (1981): 447-459.Cornell, R. W. "Compliance and stress sensitivity of spur gear teeth." Journal of Mechanical Design 103, no. 2 (1981): 447-459.

[6] Kasuba, R., and Jt W. Evans. "An extended model for determining dynamic loads in spur gearing." Journal of mechanical design 103, no. 2 (1981): 398-409.

[7] Yang, D. C. H., and J. Y. Lin. "Hertzian damping, tooth friction and bending elasticity in gear impact dynamics." Journal of mechanisms, transmissions, and automation in design 109, no. 2 (1987): 189-196.

[8] Agosto, Frederick A. Just. "Damage detection based on the geometric interpretation of the eigenvalue problem." PhD diss., Ph. D. Thesis, 1997.

[9] Tian, Xinhao. "Dynamic simulation for system response of gearbox including localized gear faults." PhD diss., University of Alberta, 2004.

[10] Wu, Siyan, Ming J. Zuo, and Anand Parey. "Simulation of spur gear dynamics and estimation of fault growth." Journal of Sound and Vibration 317, no. 3-5 (2008): 608-624.

[11] Pandya, Yogesh, and Anand Parey. "Simulation of crack propagation in spur gear tooth for different gear parameter and its influence on mesh stiffness." Engineering Failure Analysis 30 (2013): 124-137.

[12] Pandya, Yogesh, and Anand Parey. "Failure path based modified gear mesh stiffness for spur gear pair with tooth root crack." Engineering Failure Analysis 27 (2013): 286-296.

[13] Chaari, Fakher, Tahar Fakhfakh, and Mohamed Haddar. "Analytical modelling of spur gear tooth crack and influence on gearmesh stiffness." European Journal of Mechanics-A/Solids28, no. 3 (2009): 461-468.

[14] Zhou, Xiaojun, Yimin Shao, Yaguo Lei, and Mingjian Zuo. "Time-varying meshing stiffness calculation and vibration analysis for a 16DOF dynamic model with linear crack growth in a pinion." Journal of Vibration and Acoustics 134, no. 1 (2012): 011011.

[15] Chen, Zaigang, and Yimin Shao. "Dynamic simulation of spur gear with tooth root crack propagating along tooth width and crack depth." Engineering Failure Analysis 18, no. 8 (2011): 2149-2164.

[16] Mohammed, Omar D., Matti Rantatalo, and Jan-Olov Aidanpää. "Improving mesh stiffness calculation of cracked gears for the purpose of vibration-based fault analysis." Engineering Failure Analysis 34 (2013): 235-251.

[17] Wang, Liming, and Yimin Shao. "Fault mode analysis and detection for gear tooth crack during its propagating process based on dynamic simulation method." Engineering Failure Analysis 71 (2017): 166-178.

[18] Chen, Zaigang, Jie Zhang, Wanming Zhai, Yawen Wang, and Jianxin Liu. "Improved analytical methods for calculation of

gear tooth fillet-foundation stiffness with tooth root crack." Engineering Failure Analysis 82 (2017): 72-81.

[19] Wu, Jiateng, Yu Yang, Xingkai Yang, and Junsheng Cheng. "Fault feature analysis of cracked gear based on LOD and analytical-FE method." Mechanical Systems and Signal Processing 98 (2018): 951-967.

[20] Mohammed, Omar D., and Matti Rantatalo. "Gear tooth crack detection using dynamic response analysis." Insight (Northampton) 55, no. 8 (2013): 417-421.

[21] Sainsot, Philippe, Philippe Velex, and Olivier Duverger. "Contribution of gear body to tooth deflections—a new bidimensional analytical formula." Journal of mechanical design 126, no. 4 (2004): 748-752.

[22] Tada, Hiroshi, Paul C. Paris, and George R. Irwin. "The stress analysis of cracks." Handbook, Del Research Corporation(1973).

[23] Mohammed, Omar D., Matti Rantatalo, and Uday Kumar. "Analytical crack propagation scenario for gear teeth and time-varying gear mesh stiffness." vol 6 (2012): 1106-1111.